Journal of Civil Engineering Researchers

J-Researchers

JOURNAL OF CIVIL ENGINEERING RESEARCHERS

Evaluation of Modified Seismic Model Using Shear Keys at Steel Beam Connections to Concrete Colum

Lobat Hosseinzadeh[a*]

[a]*PHD Student of civil engineering,Islamic Azad University,Chaloos Branch,Iran*

Article History: Received date 2022.02.05; revised date : 2022.03.10; accepted 2022.05.24

Abstract

Reinforced concrete columns to steel beam connections are recently considered as structural system. This system takes the advantages of both through optimally combining metal and concrete structural elements. There are two connections through beam and through column connections. This study first reviewed the literature; then, the authors modeled a sample connection experimentally carried out in a laboratory by Cheng Chih and Cheng Tung Chen in 2005 by ABAQUS finite element software and investigated seismic performance of RCS connections under back/forward and monotonic loadings. Once the finite element model was validated, a parametric study (studying web steel panel thickness at the joint, studying coating thickness, etc.) was conducted; and finally, a modified model was proposed following connection results were compared showing a more stable and desired behavior in addition to the increased capacity of the connections. The result showed that the use of a through-plate with shear keys in the joint zone will increase the strength of the joint and the formation of a plastic joint outside the joint and will greatly improve the joint behavior. So that the contribution of concrete in the shear capacity of this area has increased, which was 73% for the modified model of Cheng and Chen. Also the use of a through-plate for RCS joints converts the forces transmitted from the beam to in-plane stresses and by shear keys, through two shear and support mechanisms, these forces are transferred to the concrete of the joint area and in consequence, these stresses are transferred to the concrete column.

Key terms: Steel beam connection to concrete column, Finite element method (FEM), RCS

1. Introduction

Numerical modeling is a widely economical time-saving applied technique to solve complex problems [1, 2]. In recent years, RCS systems, as one of the new building systems consisting of the

reinforced concrete columns and steel beams, have been widely considered in the design and construction of buildings in the United States and Japan [3]. In Japan large construction companies have developed their facilities and invested in research on RCS systems. As a result, a large number of beam-to-column details have been proposed to implement this system so far [4-6]. These systems are typically based on standards published by the Japan Institute of Architecture [7] and the Japan Building Center (BCJ). 1994) However, most of the new details of these connections are not covered by the standards. Developing basic design methods for RCS systems and connections is an urgent need in Japan. The study of the interconnection of RCS systems included the study of "composite and hybrid structures" as part of a joint US-Japanese seismic research program that began in April 1993 as a five-year research program [8]. Numerous experimental studies have been performed to study the performance of RCS. Sheikh, Deierlein, Yura and Jirsa [9] tested RCS internal connections on a scale of 3.2 at the University of Texas. RCS connections have also been tested by KANNNO [10] at Cornell University. Kim and Noguchi [11] studied the shear strength of RCS joints in detail through finite element analysis. To estimate the shear strength of RCS internal and external joints, experimental research including 9 RCS external joints was performed at the University of Michigan [12, 13].

Cheng and Chen [14] tested six RCS connections by considering different parameters such as Connection stirrups, beam cross-section effects and loading protocol. All research on this type of composite structure up to 2011 was reviewed by Li, Li, Jiang and Jiang [15]. Noguchi and Uchida [16] investigated two RCS frames focusing on connection failure and investigating connection mechanism states through nonlinear FEM analysis. Li, Li and Jiang [17] proposed a model and conducted a parametric study to investigate the behavior of composite concrete columns by continuous compound spiral ties and enclosed steel beams. Alizadeh, Attari and Kazemi [18] tested two new cases of RCS internal connections based on the strong column weak-beam (SCWB) criterion to study the performance of new details for RCS connections.

Xu, Fan, Lu and Li [19] proposed a new type of pre-pressed spring self-centering energy dissipation system (PS-SCED) that combines friction mechanisms between internal and external pipe components for energy supply. Cao, Feng and Wu [20] studied the seismic performance of reinforced concrete frames (RC) reinforced by steel bracing, which considers the effect of filler walls. Since the implementation of RCS connections of the through-beam is stronger than the connections of the through-column, therefore, in this research, a model will be investigated that in addition to ease of implementation, the resistance of the connection is not less than the connections of the beam type.

2. the Experiment conducted by Cheng Chih Chen and Chin Tun Chen

In this study, the seismic behavior of steel beam to the concrete slab and non-slab column connection was evaluated in National Center for Research on Earthquake Engineering (NCREE), Taiwan. A total of six cross-shaped connections were made and evaluated. All experimental samples were the same size with steel beams of H596×199×10×15 and a 65×65cm concrete column. According to load combining, beam sizes of the roof to the first floor were H596×199×10×15,H396×199×7×11,and,H500×200×10×16,respectively (samples of all tests were for the first floor). The concrete column was reinforced by 12 longitudinal rebar in #11.

Figure 1 represents the experiment. Prior to the experiment, a hydraulic jack imposes a fixed 1000 kN axial load over the column indicating the gravity load obtained by frame analysis. Then, the hydraulic drivers, at both beam ends, impose a cyclic load, as shown in Figure 2, through a triangular applied displacement. During the experiment, a horizontal driver at the top of the column keeps the column in the current state and only allows for in-plate rotation.

[3]

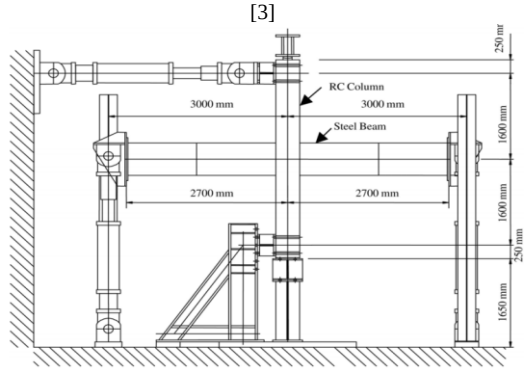

Figure 1: Schematic of experimental set up [3]

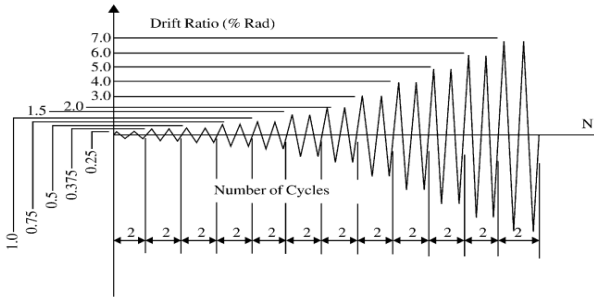

Figure 2: backward/forward displacement graph on beam ends

3. Finite element modeling through ABAQUS

ABAQUS was produced by ABAQUS Company, of active finite element software firms, in 1987. In the implicit nonlinear static analysis, the software applied two Static General and Static Rik's procedure analysis methods. This research used the nonlinear static general analysis method by Newton-Raphson convergence algorithm.

The initial development value for analysis is 0.001, the minimum development value is equal to a small value of 10-10 × 1, the maximum number of samples per step is 10,000 and the selection of samples is selected automatically.

3.1 Concrete compressive stress-strain curve

This graph is determined based on concrete uniaxial compressive test results. Three areas of the graph are introduced for under pressure concrete. The first part is assumed elastic to the load and resistance factor (LRF) stress, which is [4], where is the concrete compressive strength. strain associated to the stress is 0.0022. Young's modulus is also calculated by [4] and the Poisson ratio is 0.2. The second part, which is parabolic starts from LRF stress point up to reaching the highest concrete compressive strength, . It is obtained as follows:

$$\sigma_c = \left(\frac{kn - n^2}{1 + (k-2)n} \right) f_{ck} \quad (1)$$

Where,

$$\varepsilon_{c1} = 0.0022 \qquad k = 1.1 E_{cm} \times \frac{\varepsilon_{c1}}{f_{ck}} \qquad n = \frac{\varepsilon_c}{\varepsilon_{c1}} \quad (2)$$

Where, E_{cm} is the concrete elasticity modulus.

The third part of stress-strain curve is the descending graph from f_c to rf_c, where r is 0.85. Concrete ultimate strain (ε_{cu}) in stress failure rf_c equals 0.01.

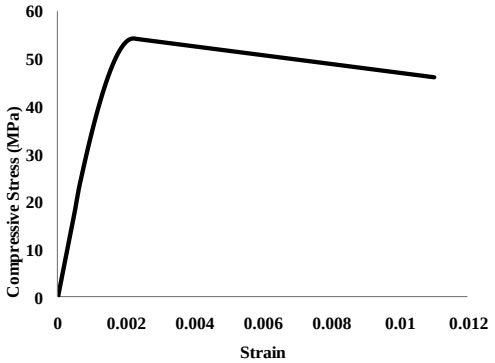

Figure 4: Concrete strain-stress curve at the compressive strength of f'_c =54Mpa

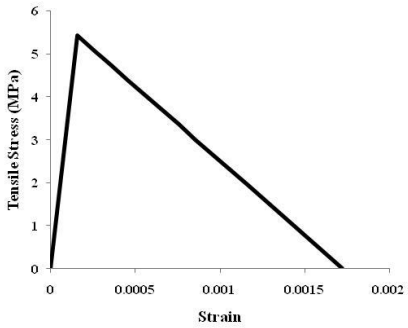

Figure 3: Concrete tensile stress-strain curve at compressive strength f'_c =54Mpa

3.2Steel materials

The two-line Elasto-plastic model is used for steel beams and rebar. Further, a similar behavior was also assumed for both strain and stress .

4. Boundary conditions

Concrete column, in the laboratory tests, belongs to the first floor jointed to foundation by a clamped connection. Therefore, in modeling, all translational and rotational column degrees of freedom U_1, U_2 , U_3 , UR_1 , UR_2 , UR_3 connected to the rigid plate anchor are also closed. Indeed, this boundary condition is applied to the rigid plate reference point influenced other nodes. In the laboratory test, a hydraulic driver keeps the column current status prior to testing such that it is only allowed in-plate rotation. In software, only UR2 degree of freedom is open to simulate upstream column boundary conditions. The beams, at both ends, may move upward and downward rotating in-plate. In the finite element model, at beam ends, only U3 and UR_2 degrees of freedom are open; while, U_1, U_2 , UR_1 , and UR_3 are close.

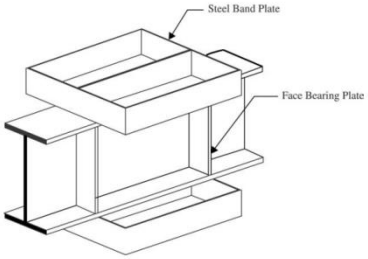

Figure 5: Steel connection including the beam and trace sheets [3]

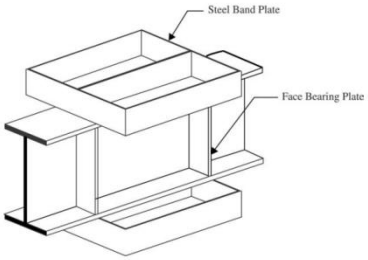

Figure 5: Steel connection including the beam and trace sheets [3]

5. Size and types of elements

The concrete column was modeled by 3D C3D8R elements accessed in ABAQUS library, which are, in fact, 8-point elements used for non-linear analyses including contacting two bodies, large deformations, plasticity, and failure. Steel beams and other connected components were also meshed by the elements. Rebar and anchor rigid plates were also modeled by T3D2 and R3D4 truss elements, respectively. In addition, to decrease analysis time, larger elements were mostly used and smaller elements were used in connection zones. Elements, in most beam and column zones, were 35 mm; while, the smallest was 18 mm.

6. Results of finite element analysis and INUC experimental results

As seen in Figure 7, numerical and experimental results were consistent in drifts smaller than 4% showing consistently similar behavior. They experience the maximum resistance at drift 4%; whereas, at higher drifts, the resistance may not

drop and is constantly up to the drift of 7% as the steel behavioral model was elasto-plastic in the finite element model with no failure. However, in the laboratory model, the resistance is dropped at higher cycles, once the resistance reaches the maximum of 4%.

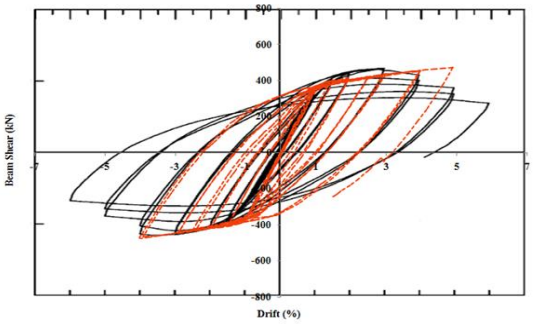

Figure 7: Comparison of beam shear graph to beam end displacement in FE and laboratory models

6.1 Main stress distribution of minimum connection

Connection shear resistance is measured based on concrete connection effective width, which is total width of inner and outer panel. Inner zone concrete is activated against the bruise of anchor plates and beam wings. Concrete presence outside beam wings range depends on activation of horizontal pressure pickets formed by double sheets bruising and or steel column on the concrete up and down the connection. Pressure shaft at the compressive picket end is dealt with beam up and down horizontal controls. Up and down beam controllers are required to deal with beam horizontal and perpendicular tensile forces. Beam perpendicular forces are balanced and beam parallel forces are transferred to the outer compression zone. This section tried to represent the mechanisms formed in concrete inner and outer connection of finite element results. Figure 8 clearly shows how these mechanisms are formed.

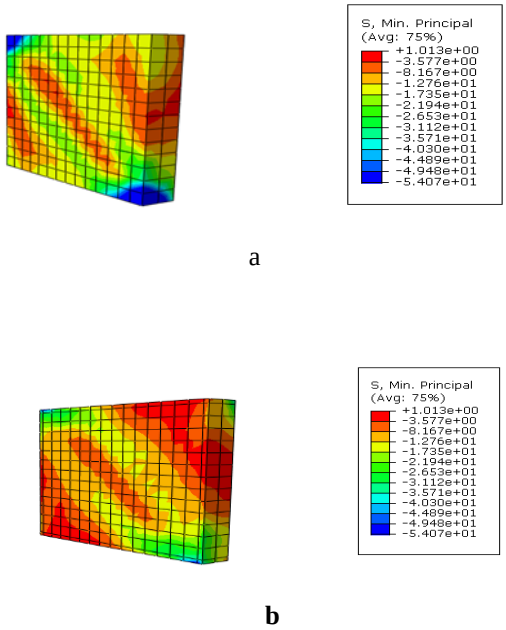

Figure 8: Diagonal compressive pickets in a. inner concrete panel, b. outer concrete panel

7. Modified model

In this model, Cheng and Chen's model is modified such that beam wings are removed at connection zone; and the middle plate extends out the connection by adding cross-beam effect; the beam is connected to the connection by welding beam web and wing to the middle plate, as seen in Figure 15. Moreover, the middle plate is designed such that middle plate cross-section is larger than beam plastic cross-section (Z_p); and consequently, the plastic joint is transferred out the connection. Hence, middle plate thickness is 20 mm. In addition, beam effect perpendicular to beam main axis is regarded considering perpendicular steel panel. Thus, connection zone is turned into four springs, where five rows of L-shaped plates were used (see Figure 9b). Furthermore, the stirrups of joint zone is removed and SCP plates of 15 mm thickness are used instead of SBP.

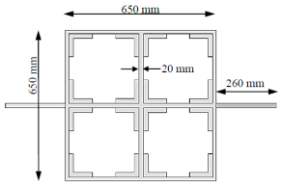

a. Connection steel characterization

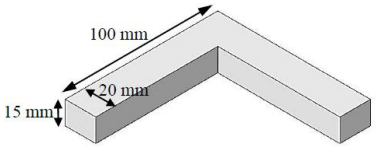

b. Specification of shear keys

7.1 Evaluation of the proposed bonding strength comparing Cheng and Chen model

Comparing the results of Cheng and Chen and the proposed modified model revealed that shear responses are larger than the proposed model drift in terms of hardness and strength. Finite element model responses for Cheng and Chen and the proposed model by middle plate and shear keys under unilateral uniform loading are shown in Figure 10.

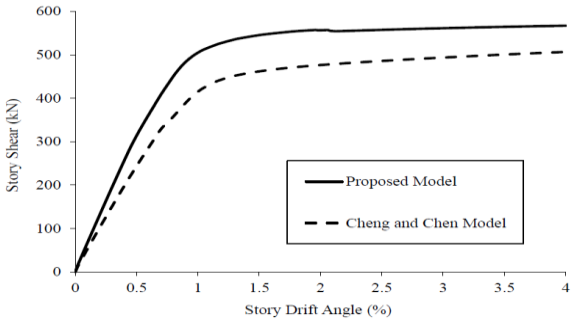

Figure 10: Finite element model responses versus uniform loading for Cheng and Chen and the proposed models

7.2 Stress distribution in a middle plate and shear keys

As Cheng and Chen considered drift of 1.4%, the modified model used this drift to study the mechanisms, too. At drift 1.4%, web steel plate approaches the yield tension from the middle zone; by drift gradual increase, most zones reaches to the yield tension. Since the joint zone is properly reinforced, steel beam web tensions reach the yield threshold at the middle connection zone; however, plastic joint is not formed in the connection. Figure 11 represents path tension distribution contours in steel beam web at drift 1.4%.

7.3Tension distribution in concrete junction

As seen in Figure 18, concrete junction is activated versus bruising of shear keys and SCP plates. Activation of concrete junction depends on two friction factors between steel and concrete considered by shear keys. In general, the friction coefficient is increased leading to better simulation and compressive picket at concrete junction. SCP is the second factor, which helps in forming concrete picket at the junction and better circulation of the forces. This section tried to show concrete junction mechanisms of the finite element model. Figure 12 illustrates how this mechanism is formed.

7.4 Studying plastic joint mechanism

As previously mentioned, new connection is designed such that the plastic joint is formed inside and no inside connection reaches up to the yielding threshold. This is a desired mechanism as structure repair and rehabilitation are enabled following beam plasticization. While, if it occurs inside the connection, it would be impossible to repair and rehabilitate the structure. The proposed model analysis showed that plastic strains are formed inside beam elements clearly indicating plastic joints in the beams. However, wing buckling, as seen in Figure 13, occurs at the compressive wing.

7.5 Cracking in concrete column

In this model, as displacement is applied to the beam ends, like Cheng and Chen model, and regarding that the column is only allowed to in-plate rotation (one clamped end), the rotation is small which causes little damage to the column and few cracks at concrete column junction. In addition, transverse cracks occur just above and below steel

beam. Figure 14 shows cracking finite element analysis results, which are few.

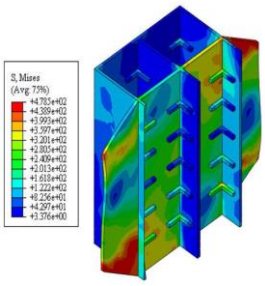

Figure 11: Mises tension distribution contours in the middle plate and shear keys at drift 1.4%

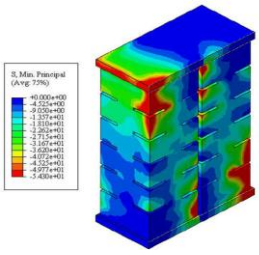

Figure 12: Minimum main tension distribution contour at concrete junction

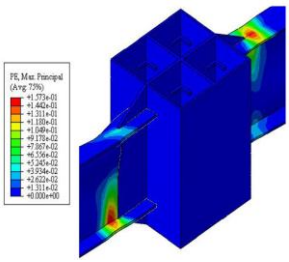

Figure 13: Plastic strain distribution contour at steel zone

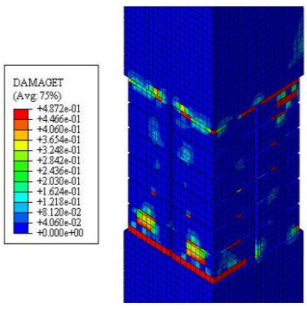

Figure 14: Concrete cracking distribution contour

7.6 Various force elements at junction

Therefore, according to Table 1, junction shearing contribution of various elements is obtained by finite element analysis results through ABAQUS at drift 1.4% is:

Table 1: Share of various force elements at junction at drift 1.4%

Middle plate panel	231 KN
Concrete junction contribution	655 KN
Junction shear capacity	889 KN
The force created in the concrete picket	1976 KN

8. Conclusion

1. Beam and column set is transformed by four components including beam bending, column bending, joint crushing, and connection panel shearing.
2. Connection is divided into three shear resistance components: steel web panel, internal concrete panel, and external concrete panel. All these components are activated against shear force. Steel panel firstly yields; next, shear capacity of web steel panel slowly increases. And then, indoor and outdoor concrete panels resist against shear force.
3. Applying middle plate with shear keys at junction causes increased connection resistance and plastic joint outside connection and largely improves connection behavior. Therefore, junction concrete contribution in shear capacity increases at this zone, which is 90% for Nishiyama and Kuramoto model and 73% for Cheng and Chin.
4. Middle plate for RCS connections turn to beam transferred forces into in-plate tension; then, the forces are transferred to concrete junction through shear and anchor mechanisms by shear keys. However, the tensions are consequently transferred to the concrete column.

References

[1] H.H. Asli, M. Arabani, Analysis of Strain and Failure of Asphalt Pavement, Computational Research Progress in Applied Science & Engineering 08(01) (2022).

[2] M. Feizbahr, C. Kok Keong, F. Rostami, M. Shahrokhi, Wave energy dissipation using perforated and non perforated piles, International Journal of Engineering 31(2) (2018) 212-219.

[3] A. Joorabchian, Z. Li, K.D. Peterman, Experimental and numerical investigation of fixed-height cold-formed steel wall assemblies bearing on concrete slabs, Thin-Walled Structures 166 (2021) 107940.

[4] A.I.o.J. (AIJ), Proc., Symp. on Mechanical Behavior of Beam to Column Connections for Composite RCS Systems, Tokyo, Japan, 1994.

[5] S. Ghods, A. Kheyroddin, M. Nazeryan, S.M. Mirtaheri, M. Gholhaki, Nonlinear behavior of connections in RCS frames with bracing and steel plate shear wall, Steel and Composite Structures 22(4) (2016) 915-935.

[6] S.M. Mirtaheri, M. Nazeryan, M.K. Bahrani, A. Nooralizadeh, L. Montazerian, M. Naserifard, Local and global buckling condition of all-steel buckling restrained braces, Steel Compos. Struct 23(2) (2017) 217-228.

[7] A. AIJ, Standards for Structural Calculation of Steel Reinforced Concrete Structures, Architectural Institute of Japan (2001).

[8] H. Yamanouchi, 'US–Japan cooperative structural research project on composite and hybrid structure. Part 1: Overall research program, Summaries, Technical Papers of Annual Meeting, Architectural Inst., Jpn, 1994, pp. 1521-1522.

[9] T.M. Sheikh, G.G. Deierlein, J.A. Yura, J.O. Jirsa, Beam-column moment connections for composite frames: Part 1, Journal of Structural Engineering 115(11) (1989) 2858-2876.

[10] R. KANNNO, Strength, deformation, and seismic resistance of joints between steel beams and reinforced concrete columns, Doctor Dissertation presented to the Faculty of Graduate School of Cornell University (1993).

[11] K. Kim, H. Noguchi, A study on the ultimate shear strength of connections with RC columns and steel beams, J. Struct. Construct. Eng 507 (1998) 163-169.

[12] G. Parra-Montesinos, J.K. Wight, Seismic response of exterior RC column-to-steel beam connections, Journal of structural engineering 126(10) (2000) 1113-1121.

[13] G. Parra-Montesinos, J.K. Wight, Modeling shear behavior of hybrid RCS beam-column connections, Journal of Structural Engineering 127(1) (2001) 3-11.

[14] C.-T. Cheng, C.-C. Chen, Seismic behavior of steel beam and reinforced concrete column connections, Journal of constructional steel research 61(5) (2005) 587-606.

[15] W. Li, Q.-n. Li, W.-s. Jiang, L. Jiang, Seismic performance of composite reinforced concrete and steel moment frame structures–state-of-the-art, Composites Part B: Engineering 42(2) (2011) 190-206.

[16] H. Noguchi, K. Uchida, Finite element method analysis of hybrid structural frames with reinforced concrete columns and steel beams, Journal of structural engineering 130(2) (2004) 328-335.

[17] W. Li, Q.-n. Li, W.-s. Jiang, Parameter study on composite frames consisting of steel beams and reinforced concrete columns, Journal of Constructional Steel Research 77 (2012) 145-162.

[18] S. Alizadeh, N.K. Attari, M. Kazemi, The seismic performance of new detailing for RCS connections, Journal of constructional steel research 91 (2013) 76-88.

[19] L.-H. Xu, X. Fan, D. Lu, Z.-X. Li, Hysteretic behavior studies of self-centering energy dissipation bracing system, Steel and Composite Structures 20(6) (2016) 1205-1219.

[20] P. Cao, N. Feng, K. Wu, Experimental study on infilled frames strengthened by profiled steel sheet bracing, Steel and Composite Structures 17(6) (2014) 777-790.